

Search for a strangeonium-like structure Z_s decaying into $\phi\pi$ and a measurement of the cross section $e^+e^- \rightarrow \phi\pi\pi$

M. Ablikim¹, M. N. Achasov^{9,d}, S. Ahmed¹⁴, M. Albrecht⁴, A. Amoroso^{53A,53C}, F. F. An¹, Q. An^{50,40}, J. Z. Bai¹, Y. Bai³⁹, O. Bakina²⁴, R. Baldini Ferroli^{20A}, Y. Ban³², D. W. Bennett¹⁹, J. V. Bennett⁵, N. Berger²³, M. Bertani^{20A}, D. Bettoni^{21A}, J. M. Bian⁴⁷, F. Bianchi^{53A,53C}, E. Boger^{24,b}, I. Boyko²⁴, R. A. Briere⁵, H. Cai⁵⁵, X. Cai^{1,40}, O. Cakir^{43A}, A. Calcaterra^{20A}, G. F. Cao^{1,44}, S. A. Cetin^{43B}, J. Chai^{53C}, J. F. Chang^{1,40}, G. Chelkov^{24,b,c}, G. Chen¹, H. S. Chen^{1,44}, J. C. Chen¹, M. L. Chen^{1,40}, P. L. Chen⁵¹, S. J. Chen³⁰, X. R. Chen²⁷, Y. B. Chen^{1,40}, X. K. Chu³², G. Cibinetto^{21A}, H. L. Dai^{1,40}, J. P. Dai^{35,h}, A. Dbeyssi¹⁴, D. Dedovich²⁴, Z. Y. Deng¹, A. Denig²³, I. Denysenko²⁴, M. Destefanis^{53A,53C}, F. De Mori^{53A,53C}, Y. Ding²⁸, C. Dong³¹, J. Dong^{1,40}, L. Y. Dong^{1,44}, M. Y. Dong^{1,40,44}, Z. L. Dou³⁰, S. X. Du⁵⁷, P. F. Duan¹, J. Fang^{1,40}, S. S. Fang^{1,44}, Y. Fang¹, R. Farinelli^{21A,21B}, L. Fava^{53B,53C}, S. Fegan²³, F. Feldbauer²³, G. Felici^{20A}, C. Q. Feng^{50,40}, E. Fioravanti^{21A}, M. Fritsch^{23,14}, C. D. Fu¹, Q. Gao¹, X. L. Gao^{50,40}, Y. Gao⁴², Y. G. Gao¹, Z. Gao^{50,40}, I. Garzia^{21A}, K. Goetzen¹⁰, L. Gong³¹, W. X. Gong^{1,40}, W. Gradl²³, M. Greco^{53A,53C}, M. H. Gu^{1,40}, Y. T. Gu¹², A. Q. Guo¹, R. P. Guo^{1,44}, Y. P. Guo²³, Z. Haddadi²⁶, S. Han⁵⁵, X. Q. Hao¹⁵, F. A. Harris⁴⁵, K. L. He^{1,44}, X. Q. He⁴⁹, F. H. Heinsius⁴, T. Held⁴, Y. K. Heng^{1,40,44}, T. Holtmann⁴, Z. L. Hou¹, H. M. Hu^{1,44}, T. Hu^{1,40,44}, Y. Hu¹, G. S. Huang^{50,40}, J. S. Huang¹⁵, X. T. Huang³⁴, X. Z. Huang³⁰, Z. L. Huang²⁸, T. Hussain⁵², W. Ikegami Andersson⁵⁴, Q. Ji¹, Q. P. Ji¹⁵, X. B. Ji^{1,44}, X. L. Ji^{1,40}, X. S. Jiang^{1,40,44}, X. Y. Jiang³¹, J. B. Jiao³⁴, Z. Jiao¹⁷, D. P. Jin^{1,40,44}, S. Jin^{1,44}, Y. Jin⁴⁶, T. Johansson⁵⁴, A. Julin⁴⁷, N. Kalantar-Nayestanaki²⁶, X. L. Kang¹, X. S. Kang³¹, M. Kavatsyuk²⁶, B. C. Ke⁵, T. Khan^{50,40}, A. Khoukaz⁴⁸, P. Kiese²³, R. Kliemt¹⁰, L. Koch²⁵, O. B. Kolcu^{43B,f}, B. Kopf⁴, M. Kornicer⁴⁵, M. Kuemmel⁴, M. Kuessner⁴, M. Kuhlmann⁴, A. Kupsc⁵⁴, W. Kühn²⁵, J. S. Lange²⁵, M. Lara¹⁹, P. Larin¹⁴, L. Lavezzi^{53C}, H. Leithoff²³, C. Leng^{53C}, C. Li⁵⁴, Cheng Li^{50,40}, D. M. Li⁵⁷, F. Li^{1,40}, F. Y. Li³², G. Li¹, H. B. Li^{1,44}, H. J. Li⁴⁴, J. C. Li¹, Jin Li³³, K. J. Li⁴¹, Kang Li¹³, Ke Li³⁴, Lei Li³, P. L. Li^{50,40}, P. R. Li^{44,7}, Q. Y. Li³⁴, W. D. Li^{1,44}, W. G. Li³⁴, X. N. Li^{1,40}, X. Q. Li³¹, Z. B. Li⁴¹, H. Liang^{50,40}, Y. F. Liang³⁷, Y. T. Liang²⁵, G. R. Liao¹¹, D. X. Lin¹⁴, B. Liu^{35,h}, B. J. Liu¹, C. X. Liu¹, D. Liu^{50,40}, F. H. Liu³⁶, Fang Liu¹, Feng Liu⁶, H. B. Liu¹², H. M. Liu^{1,44}, Huanhuan Liu¹, Huihui Liu¹⁶, J. B. Liu^{50,40}, J. P. Liu⁵⁵, J. Y. Liu^{1,44}, K. Liu⁴², K. Y. Liu²⁸, Ke Liu⁶, L. D. Liu³², P. L. Liu^{1,40}, Q. Liu⁴⁴, S. B. Liu^{50,40}, X. Liu²⁷, Y. B. Liu³¹, Z. A. Liu^{1,40,44}, Zhiqing Liu²³, Y. F. Long³², X. C. Lou^{1,40,44}, H. J. Lu¹⁷, J. G. Lu^{1,40}, Y. Lu¹, Y. P. Lu^{1,40}, C. L. Luo²⁹, M. X. Luo⁵⁶, X. L. Luo^{1,40}, X. R. Lyu⁴⁴, F. C. Ma²⁸, H. L. Ma¹, L. L. Ma³⁴, M. M. Ma^{1,44}, Q. M. Ma¹, T. Ma¹, X. N. Ma³¹, X. Y. Ma^{1,40}, Y. M. Ma³⁴, F. E. Maas¹⁴, M. Maggiora^{53A,53C}, Q. A. Malik⁵², Y. J. Mao³², Z. P. Mao¹, S. Marcello^{53A,53C}, Z. X. Meng⁴⁶, J. G. Messchendorp²⁶, G. Mezzadri^{21B}, J. Min^{1,40}, T. J. Min¹, R. E. Mitchell¹⁹, X. H. Mo^{1,40,44}, Y. J. Mo⁶, C. Morales Morales¹⁴, N. Yu. Muchnoi^{9,d}, H. Muramatsu⁴⁷, A. Mustafa⁴, Y. Nefedov²⁴, F. Nerling¹⁰, I. B. Nikolaev^{9,d}, Z. Ning^{1,40}, S. Nisar⁸, S. L. Niu^{1,40}, X. Y. Niu^{1,44}, S. L. Olsen^{33,j}, Q. Ouyang^{1,40,44}, S. Pacetti^{20B}, Y. Pan^{50,40}, M. Papenbrock⁵⁴, P. Patteri^{20A}, M. Pelizaeus⁴, J. Pellegrino^{53A,53C}, H. P. Peng^{50,40}, K. Peters^{10,g}, J. Pettersson⁵⁴, J. L. Ping²⁹, R. G. Ping^{1,44}, A. Pitka²³, R. Poling⁴⁷, V. Prasad^{50,40}, H. R. Qi², M. Qi³⁰, S. Qian^{1,40}, C. F. Qiao⁴⁴, N. Qin⁵⁵, X. S. Qin⁴, Z. H. Qin^{1,40}, J. F. Qiu¹, K. H. Rashid^{52,i}, C. F. Redmer²³, M. Richter⁴, M. Ripka²³, M. Rolo^{53C}, G. Rong^{1,44}, Ch. Rosner¹⁴, A. Sarantsev^{24,e}, M. Savrié^{21B}, C. Schnier⁴, K. Schoenning⁵⁴, W. Shan³², M. Shao^{50,40}, C. P. Shen², P. X. Shen³¹, X. Y. Shen^{1,44}, H. Y. Sheng¹, J. J. Song³⁴, W. M. Song³⁴, X. Y. Song¹, S. Sosio^{53A,53C}, C. Sowa⁴, S. Spataro^{53A,53C}, G. X. Sun¹, J. F. Sun¹⁵, L. Sun⁵⁵, S. S. Sun^{1,44}, X. H. Sun¹, Y. J. Sun^{50,40}, Y. K. Sun^{50,40}, Y. Z. Sun¹, Z. J. Sun^{1,40}, Z. T. Sun¹⁹, C. J. Tang³⁷, G. Y. Tang¹, X. Tang¹, I. Tapan^{43C}, M. Tiemens²⁶, B. Tsednee²², I. Uman^{43D}, G. S. Varner⁴⁵, B. Wang¹, B. L. Wang⁴⁴, D. Wang³², D. Y. Wang³², Dan Wang⁴⁴, K. Wang^{1,40}, L. L. Wang¹, L. S. Wang¹, M. Wang³⁴, Meng Wang^{1,44}, P. Wang¹, P. L. Wang¹, W. P. Wang^{50,40}, X. F. Wang⁴², Y. Wang³⁸, Y. D. Wang¹⁴, Y. F. Wang^{1,40,44}, Y. Q. Wang²³, Z. Wang^{1,40}, Z. G. Wang^{1,40}, Z. Y. Wang¹, Zongyuan Wang^{1,44}, T. Weber²³, D. H. Wei¹¹, P. Weidenkaff²³, S. P. Wen¹, U. Wiedner⁴, M. Wolke⁵⁴, L. H. Wu¹, L. J. Wu^{1,44}, Z. Wu^{1,40}, L. Xia^{50,40}, Y. Xia¹⁸, D. Xiao¹, H. Xiao⁵¹, Y. J. Xiao^{1,44}, Z. J. Xiao²⁹, Y. G. Xie^{1,40}, Y. H. Xie⁶, X. A. Xiong^{1,44}, Q. L. Xiu^{1,40}, G. F. Xu¹, J. J. Xu^{1,44}, L. Xu¹, Q. J. Xu¹³, Q. N. Xu⁴⁴, X. P. Xu³⁸, L. Yan^{53A,53C}, W. B. Yan^{50,40}, W. C. Yan², Y. H. Yan¹⁸, H. J. Yang^{35,h}, H. X. Yang¹, L. Yang⁵⁵, Y. H. Yang³⁰, Y. X. Yang¹¹, M. Ye^{1,40}, M. H. Ye⁷, J. H. Yin¹, Z. Y. You⁴¹, B. X. Yu^{1,40,44}, C. X. Yu³¹, J. S. Yu²⁷, C. Z. Yuan^{1,44}, Y. Yuan¹, A. Yuncu^{43B,a}, A. A. Zafar⁵², Y. Zeng¹⁸, Z. Zeng^{50,40}, B. X. Zhang¹, B. Y. Zhang^{1,40}, C. C. Zhang¹, D. H. Zhang¹, H. H. Zhang⁴¹, H. Y. Zhang^{1,40}, J. Zhang^{1,44}, J. L. Zhang¹, J. Q. Zhang¹, J. W. Zhang^{1,40,44}, J. Y. Zhang¹, J. Z. Zhang^{1,44}, K. Zhang^{1,44}, L. Zhang⁴², S. Q. Zhang³¹, X. Y. Zhang³⁴, Y. H. Zhang^{1,40}, Y. T. Zhang^{50,40}, Yang Zhang¹, Yao Zhang¹, Yu Zhang⁴⁴, Z. H. Zhang⁶, Z. P. Zhang⁵⁰, Z. Y. Zhang⁵⁵, G. Zhao¹, J. W. Zhao^{1,40}, J. Y. Zhao^{1,44}, J. Z. Zhao^{1,40}, Lei Zhao^{50,40}, Ling Zhao¹, M. G. Zhao³¹, Q. Zhao¹, S. J. Zhao⁵⁷, T. C. Zhao¹, Y. B. Zhao^{1,40}, Z. G. Zhao^{50,40}, A. Zhemchugov^{24,b}, B. Zheng⁵¹, J. P. Zheng^{1,40}, W. J. Zheng³⁴, Y. H. Zheng⁴⁴, B. Zhong²⁹, L. Zhou^{1,40}, X. Zhou⁵⁵, X. K. Zhou^{50,40}, X. R. Zhou^{50,40}, X. Y. Zhou¹, Y. X. Zhou¹², J. Zhu³¹, J. Zhu⁴¹, K. Zhu¹, K. J. Zhu^{1,40,44}, S. Zhu¹, S. H. Zhu⁴⁹, X. L. Zhu⁴², Y. C. Zhu^{50,40}, Y. S. Zhu^{1,44}, Z. A. Zhu^{1,44}, J. Zhuang^{1,40}, B. S. Zou¹, J. H. Zou¹

(BESIII Collaboration)

¹ Institute of High Energy Physics, Beijing 100049, People's Republic of China

² Beihang University, Beijing 100191, People's Republic of China

³ Beijing Institute of Petrochemical Technology, Beijing 102617, People's Republic of China

⁴ Bochum Ruhr-University, D-44780 Bochum, Germany

⁵ Carnegie Mellon University, Pittsburgh, Pennsylvania 15213, USA

⁶ Central China Normal University, Wuhan 430079, People's Republic of China

⁷ China Center of Advanced Science and Technology, Beijing 100190, People's Republic of China

⁸ COMSATS Institute of Information Technology, Lahore, Defence Road, Off Raiwind Road, 54000 Lahore, Pakistan

⁹ G.I. Budker Institute of Nuclear Physics SB RAS (BINP), Novosibirsk 630090, Russia

¹⁰ GSI Helmholtzcentre for Heavy Ion Research GmbH, D-64291 Darmstadt, Germany

¹¹ Guangxi Normal University, Guilin 541004, People's Republic of China

¹² Guangxi University, Nanning 530004, People's Republic of China

¹³ Hangzhou Normal University, Hangzhou 310036, People's Republic of China

- ¹⁴ Helmholtz Institute Mainz, Johann-Joachim-Becher-Weg 45, D-55099 Mainz, Germany
- ¹⁵ Henan Normal University, Xinxiang 453007, People's Republic of China
- ¹⁶ Henan University of Science and Technology, Luoyang 471003, People's Republic of China
- ¹⁷ Huangshan College, Huangshan 245000, People's Republic of China
- ¹⁸ Hunan University, Changsha 410082, People's Republic of China
- ¹⁹ Indiana University, Bloomington, Indiana 47405, USA
- ²⁰ (A)INFN Laboratori Nazionali di Frascati, I-00044, Frascati, Italy; (B)INFN and University of Perugia, I-06100, Perugia, Italy
- ²¹ (A)INFN Sezione di Ferrara, I-44122, Ferrara, Italy; (B)University of Ferrara, I-44122, Ferrara, Italy
- ²² Institute of Physics and Technology, Peace Ave. 54B, Ulaanbaatar 13330, Mongolia
- ²³ Johannes Gutenberg University of Mainz, Johann-Joachim-Becher-Weg 45, D-55099 Mainz, Germany
- ²⁴ Joint Institute for Nuclear Research, 141980 Dubna, Moscow region, Russia
- ²⁵ Justus-Liebig-Universitaet Giessen, II. Physikalisches Institut, Heinrich-Buff-Ring 16, D-35392 Giessen, Germany
- ²⁶ KVI-CART, University of Groningen, NL-9747 AA Groningen, The Netherlands
- ²⁷ Lanzhou University, Lanzhou 730000, People's Republic of China
- ²⁸ Liaoning University, Shenyang 110036, People's Republic of China
- ²⁹ Nanjing Normal University, Nanjing 210023, People's Republic of China
- ³⁰ Nanjing University, Nanjing 210093, People's Republic of China
- ³¹ Nankai University, Tianjin 300071, People's Republic of China
- ³² Peking University, Beijing 100871, People's Republic of China
- ³³ Seoul National University, Seoul, 151-747 Korea
- ³⁴ Shandong University, Jinan 250100, People's Republic of China
- ³⁵ Shanghai Jiao Tong University, Shanghai 200240, People's Republic of China
- ³⁶ Shanxi University, Taiyuan 030006, People's Republic of China
- ³⁷ Sichuan University, Chengdu 610064, People's Republic of China
- ³⁸ Soochow University, Suzhou 215006, People's Republic of China
- ³⁹ Southeast University, Nanjing 211100, People's Republic of China
- ⁴⁰ State Key Laboratory of Particle Detection and Electronics, Beijing 100049, Hefei 230026, People's Republic of China
- ⁴¹ Sun Yat-Sen University, Guangzhou 510275, People's Republic of China
- ⁴² Tsinghua University, Beijing 100084, People's Republic of China
- ⁴³ (A)Ankara University, 06100 Tandogan, Ankara, Turkey; (B)Istanbul Bilgi University, 34060 Eyup, Istanbul, Turkey; (C)Uludag University, 16059 Bursa, Turkey; (D)Near East University, Nicosia, North Cyprus, Mersin 10, Turkey
- ⁴⁴ University of Chinese Academy of Sciences, Beijing 100049, People's Republic of China
- ⁴⁵ University of Hawaii, Honolulu, Hawaii 96822, USA
- ⁴⁶ University of Jinan, Jinan 250022, People's Republic of China
- ⁴⁷ University of Minnesota, Minneapolis, Minnesota 55455, USA
- ⁴⁸ University of Muenster, Wilhelm-Klemm-Str. 9, 48149 Muenster, Germany
- ⁴⁹ University of Science and Technology Liaoning, Anshan 114051, People's Republic of China
- ⁵⁰ University of Science and Technology of China, Hefei 230026, People's Republic of China
- ⁵¹ University of South China, Hengyang 421001, People's Republic of China
- ⁵² University of the Punjab, Lahore-54590, Pakistan
- ⁵³ (A)University of Turin, I-10125, Turin, Italy; (B)University of Eastern Piedmont, I-15121, Alessandria, Italy; (C)INFN, I-10125, Turin, Italy
- ⁵⁴ Uppsala University, Box 516, SE-75120 Uppsala, Sweden
- ⁵⁵ Wuhan University, Wuhan 430072, People's Republic of China
- ⁵⁶ Zhejiang University, Hangzhou 310027, People's Republic of China
- ⁵⁷ Zhengzhou University, Zhengzhou 450001, People's Republic of China
- ^a Also at Bogazici University, 34342 Istanbul, Turkey
- ^b Also at the Moscow Institute of Physics and Technology, Moscow 141700, Russia
- ^c Also at the Functional Electronics Laboratory, Tomsk State University, Tomsk, 634050, Russia
- ^d Also at the Novosibirsk State University, Novosibirsk, 630090, Russia
- ^e Also at the NRC "Kurchatov Institute", PNPI, 188300, Gatchina, Russia
- ^f Also at Istanbul Arel University, 34295 Istanbul, Turkey
- ^g Also at Goethe University Frankfurt, 60323 Frankfurt am Main, Germany
- ^h Also at Key Laboratory for Particle Physics, Astrophysics and Cosmology, Ministry of Education; Shanghai Key Laboratory for Particle Physics and Cosmology; Institute of Nuclear and Particle Physics, Shanghai 200240, People's Republic of China
- ⁱ Government College Women University, Sialkot - 51310. Punjab, Pakistan
- ^j Currently at: Center for Underground Physics, Institute for Basic Science, Daejeon 34126, Korea

Using a data sample of e^+e^- collision data corresponding to an integrated luminosity of 108 pb^{-1} collected with the BESIII detector at a center-of-mass energy of 2.125 GeV , we study the process $e^+e^- \rightarrow \phi\pi\pi$, and search for a strangeonium-like structure Z_s decaying into $\phi\pi$. No signal is observed in the $\phi\pi$ mass spectrum around $1.4 \text{ GeV}/c^2$. Upper limits on the cross sections for Z_s production at the 90% confidence level are determined. In addition, the cross sections of $e^+e^- \rightarrow \phi\pi^+\pi^-$ and $e^+e^- \rightarrow \phi\pi^0\pi^0$ at 2.125 GeV are measured

to be $(343.0 \pm 5.1 \pm 25.1)$ pb and $(208.3 \pm 7.6 \pm 13.5)$ pb, respectively, where the first uncertainties are statistical and the second systematic.

PACS numbers: 13.25.Jx, 13.25.Gv, 13.66.Bc

A charged charmonium-like structure, $Z_c(3900)$, was observed in the $\pi^\pm J/\psi$ final states by the BESIII and Belle experiments [1, 2]. Subsequently, several analogous structures were reported and confirmed by different experiments [3–7]. These observations inspired extensive discussions of their nature, and one of the reasonable interpretations is the tetraquark state due to these structures carrying charge and prominently decaying into a pion and a conventional charmonium state [8]. More recently, the neutral partners of these charmonium-like structures were observed [9–11], which indicate the isotriplet property of these structures and hint of a new hadron spectroscopy.

By replacing the $c\bar{c}$ pair in the Z_c structure with a $s\bar{s}$, it is possible to consider an analogous Z_s structure. Similar to $Y(4260) \rightarrow J/\psi \pi^+ \pi^-$ in which the $Z_c(3900)$ was observed [1, 2], the process $\phi(2170) \rightarrow \phi \pi^+ \pi^-$ is considered as a unique place to search for the Z_s structure, as the $\phi(2170)$ is regarded as the strangeonium-like states analogy to $Y(4260)$ in charmonium sector [12]. Furthermore, the conventional isosinglet $s\bar{s}$ state decaying into $\phi\pi$ is suppressed by the conservation of isospin symmetry, while for a conventional meson composed of u, d quarks, the $\phi\pi$ decay mode is strongly suppressed by the Okubo-Zweig-Iizuka (OZI) rule [13]. Therefore, it is of interest to perform an experimental search for the strangeonium-like structure Z_s since its observation may imply the existence of an exotic state.

In this Letter, we present a search for the Z_s structure in the process $e^+e^- \rightarrow \phi\pi\pi$ using a data sample corresponding to an integrated luminosity of (108.49 ± 0.75) pb $^{-1}$ [14], taken at a center-of-mass energy of 2.125 GeV with the BESIII detector. Since the observed $Z_c(3900)$ [1, 2] and $Z_c(3885)$ [5] are close to the $D^*\bar{D}$ mass threshold and have a narrow width, we will focus on the search for a narrow width Z_s structure around the $K^*\bar{K}$ mass threshold (1.4 GeV/ c^2) in the $\phi\pi$ mass spectrum. This also allows us to test the novel scenario of the initial single pion emission mechanism (ISPE) [15].

The BESIII detector [16] is a magnetic spectrometer located at the Beijing Electron Position Collider (BEPCII), which is a double-ring e^+e^- collider with a peak luminosity of 10^{33} cm $^{-2}$ s $^{-1}$ at a center-of-mass energy of 3.773 GeV. The cylindrical core of the BESIII detector consists of a helium-based multi-layer drift chamber (MDC), a plastic scintillator time-of-flight system (TOF), and a CsI(Tl) electromagnetic calorimeter (EMC), which are all immersed in a superconducting solenoidal magnet providing a 1.0 T magnetic field. The solenoid is supported by an octagonal flux-return yoke with resistive plate counter muon identifier modules interleaved with steel. The acceptance of charged particles is 93% over 4π solid angle. The charged-particle momen-

tum resolution at 1 GeV/ c is 0.5%, and the specific energy loss (dE/dx) resolution is 6%. The EMC measures photon energies with a resolution of 2.5% (5%) at 1 GeV in the barrel (end caps) region. The time resolution of TOF is 80 ps in the barrel and 110 ps in the end caps.

The GEANT4 [17] based Monte Carlo (MC) simulation software, which includes the geometric description of the BESIII detector and the detector response, is used to determine the detection efficiencies and estimate backgrounds. To simulate the $e^+e^- \rightarrow \phi\pi\pi$ process, the lineshape reported by BaBar [18] is adopted. Intermediate states in the simulation of $e^+e^- \rightarrow \phi\pi\pi$ process are modeled according to the BESIII data as described later.

Candidate events of $e^+e^- \rightarrow \phi\pi^+\pi^-$ ($\phi \rightarrow K^+K^-$) are required to have three or four charged tracks. Charged tracks are reconstructed from hits in the MDC within the polar angle range $|\cos\theta| < 0.93$. The tracks are required to pass the interaction point within 10 cm along the beam direction and within 1 cm in the plane perpendicular to the beam. For each charged track, the TOF and the dE/dx information are combined to form particle identification (PID) confidence levels for the π, K , and p hypotheses, and the particle type with the highest confidence level is assigned to each track. Two pions with opposite charges and at least one kaon are required to be identified. A one-constraint (1C) kinematic fit is performed under the hypothesis that the $K\pi^+\pi^-$ missing mass corresponds to the kaon mass, and the corresponding χ^2 , denoted as $\chi_{1C}^2(\pi^+\pi^-KK_{\text{miss}})$, is required to be less than 10. For events with two reconstructed and identified kaons, the combination with the smaller $\chi_{1C}^2(\pi^+\pi^-KK_{\text{miss}})$ is retained.

Candidate events of $e^+e^- \rightarrow \phi\pi^0\pi^0$ ($\phi \rightarrow K^+K^-, \pi^0 \rightarrow \gamma\gamma$) are required to have one or two charged tracks and at least four photon candidates. Photon candidates are reconstructed from isolated showers in the EMC, and the corresponding energies are required to be at least 25 MeV in the barrel ($|\cos\theta| < 0.80$) or 50 MeV in the end caps ($0.86 < |\cos\theta| < 0.92$). To eliminate showers associated with charged particles, the angle between the cluster and the nearest charged track must be larger than 10 degrees. An EMC cluster timing requirement of $0 \leq t \leq 700$ ns is also applied to suppress electronic noise and energy deposits unrelated to the event. At least one kaon is required to be identified. A 1C kinematic fit is then performed under the hypothesis that the $K4\gamma$ missing mass is the kaon mass. For events with two identified kaons or more than four photons, the combination with the smallest $\chi_{1C}^2(4\gamma KK_{\text{miss}})$ is retained and required to be less than 20. The four selected photons are grouped into pairs to form π^0 mesons. Two π^0 candidates are then selected by minimizing the quantity $(M(\gamma\gamma)_1 - m_{\pi^0})^2 + (M(\gamma\gamma)_2 - m_{\pi^0})^2$, where m_{π^0} is the nomi-

nal π^0 mass from Particle Data Group (PDG) [19]. In order to select a clean sample, both $M(\gamma\gamma)_1$ and $M(\gamma\gamma)_2$ are required to be within $\pm 20 \text{ MeV}/c^2$ of m_{π^0} .

After applying the above selection criteria, the K^+K^- invariant mass, $M(K^+K^-)$, is computed using the four-momenta of the reconstructed K and K_{miss} from the kinematic fit. The $M(K^+K^-)$ spectra for the selected candidate events are shown in Figs. 1 (a) and (b), where ϕ signals are clearly seen. The Dalitz plots of the $\phi\pi^+\pi^-$ and $\phi\pi^0\pi^0$ events are shown in Figs. 2 (a) and (b), respectively, where the $M(K^+K^-)$ is required to be in the ϕ mass range, $|M(K^+K^-) - m_\phi| < 0.01 \text{ GeV}/c^2$, and m_ϕ is the nominal ϕ mass from PDG [19]. The apparent structures are from the decay processes $e^+e^- \rightarrow \phi f_0(980)$ with $f_0(980)$ decaying to $\pi^+\pi^-$ or $\pi^0\pi^0$ final states, which are also clearly indicated in the $\pi\pi$ invariant mass spectra, $M(\pi\pi)$, displayed in Figs. 2 (c) and (d).

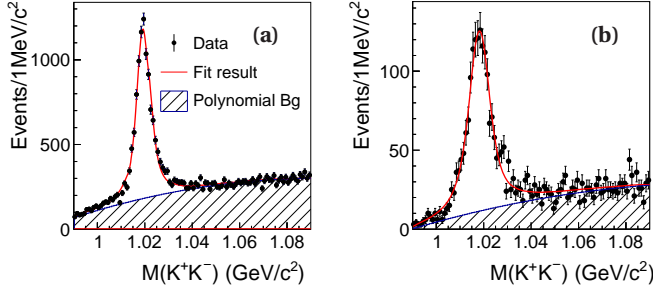


Figure 1. Invariant mass distributions of K^+K^- for (a) $e^+e^- \rightarrow K^+K^- \pi^+\pi^-$ and (b) $e^+e^- \rightarrow K^+K^- \pi^0\pi^0$ events. The dots with error bars are data, the solid lines are the fit results and the shaded parts are the combinatorial backgrounds obtained from fits.

The mass spectrum of a ϕ candidate paired with a low-momentum π (denoted as π_l) is expected to be sensitive in searching for a Z_s structure around $1.4 \text{ GeV}/c^2$. The invariant mass distributions for $\phi\pi_l^+$ and $\phi\pi_l^0$, $M(\phi\pi_l^+)$ and $M(\phi\pi_l^0)$, are shown in Fig. 3. There is no evidence of a structure around $1.4 \text{ GeV}/c^2$. In the determination of the yields of Z_s production in $e^+e^- \rightarrow \phi\pi\pi$, the contributions from non- ϕ backgrounds are described by the events in the ϕ sideband regions, $0.995 < M(K^+K^-) < 1.005$ and $1.035 < M(K^+K^-) < 1.045 \text{ GeV}/c^2$, and are normalized according to the fitted intensities in Fig. 1. The $M(\pi\pi)$ distributions of ϕ sideband events are represented by the dotted lines in Figs. 2 (c) and (d). Contributions from ρK^+K^- and ωK^+K^- are clearly seen in the $K^+K^- \pi^+\pi^-$ channel, while no obvious contribution is observed in the neutral process. In addition, $K^*(892)K^\mp\pi^\pm$ events also contaminate the charged process. The candidate events of $e^+e^- \rightarrow \phi\pi\pi$ dominantly come from the processes with intermediate states $f_0(980)$ and σ , as shown in Figs. 2 (c) and (d).

To obtain the production yields of Z_s , a good description of data without the Z_s signal is essential. Therefore, a partial wave analysis (PWA) of the $e^+e^- \rightarrow \phi\pi\pi$ candidate events

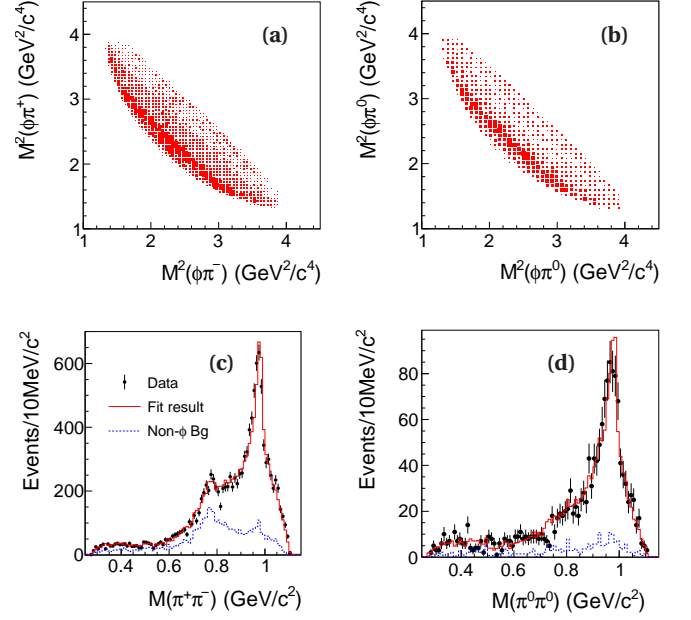


Figure 2. Dalitz plots for (a) $e^+e^- \rightarrow \phi\pi^+\pi^-$ and (b) $e^+e^- \rightarrow \phi\pi^0\pi^0$ candidate events and invariant mass distributions of (c) $\pi^+\pi^-$ and (d) $\pi^0\pi^0$. The dots with error bars are data, the dotted histograms are non- ϕ backgrounds estimated from ϕ sidebands, and the solid histograms are the sum of the projections of the PWA results and non- ϕ backgrounds. Each $e^+e^- \rightarrow \phi\pi^0\pi^0$ event contributes two entries for (b).

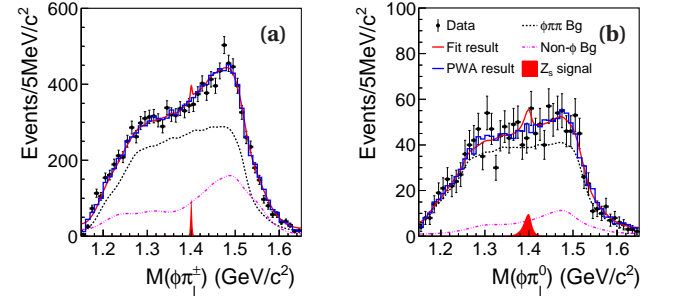


Figure 3. Invariant mass distributions of (a) $M(\phi\pi_l^+)$ and (b) $M(\phi\pi_l^0)$ for $\phi\pi\pi$ candidate events. The dots with error bars are data, the solid lines are the fit results with the numbers of Z_s fixed to the upper limits at the 90% C.L., the histograms are the projections of the PWA results and non- ϕ backgrounds, the dotted lines are the MC simulated shapes, the dash-dotted lines are non- ϕ backgrounds (estimated from ϕ sideband events), and the shaded histograms are the Z_s signal with the production rates fixed to the upper limits (three times for $\phi\pi^\pm$ to show the Z_s^\pm peak clearly).

is performed, since no obvious Z_s structure is observed. A detailed description of the PWA procedure can be found in Ref. [20]. In the fit, the $e^+e^- \rightarrow \phi\pi\pi$ process is described by four subprocesses: $e^+e^- \rightarrow \phi f_0(980)$, $\phi\sigma$, $\phi f_0(1370)$, and $\phi f_2(1270)$. The resonance parameters are fixed on the values determined in previous BES results [21, 22]. Non-

ϕ backgrounds estimated from the ϕ sidebands are represented by a non-interfering term. The projections of nominal PWA results on the $M(\pi\pi)$ distributions are shown as the solid lines in Figs. 2 (c) and (d). Based on the nominal PWA results, a dedicated MC sample is generated, which is used to explore the Z_s signal yields and estimate the detection efficiency.

Since no obvious Z_s signal is observed, the upper limit on its production is determined. A series of unbinned maximum likelihood fits to the $M(\phi\pi_l)$ distribution is performed by varying the number of Z_s signal events. In each fit, the corresponding probability density function (PDF) is a linear combination of the $\phi\pi\pi$ component described by MC simulation based on the nominal PWA results, non- ϕ backgrounds estimated from ϕ sidebands, and a MC simulated Z_s signal assuming $M(Z_s) = 1.4 \text{ GeV}/c^2$ and $\Gamma(Z_s) = 0$. The resultant normalized likelihood values as a function of the number of Z_s events are shown in Fig. 4. The upper limits N^{UL} are the number of Z_s events, $N(Z_s)$, corresponding to 90% of the area under the likelihood curves, and are determined to be 16.6 for Z_s^\pm and 25.2 for Z_s^0 at the 90% confidence level (C.L.). The corresponding fit curves with the number of Z_s signal fixed to N^{UL} are displayed as the solid lines in Fig. 3. Additionally, we also determine the upper limits with the scenario of different width and mass of Z_s , *i.e.* $\Gamma(Z_s) = 5$ or 10 MeV and $M(Z_s) = 1.38$ or 1.42 GeV/c^2 . The corresponding upper limits on the yields of Z_s signal and the detection efficiencies obtained with the phase space distributed MC sample are summarized for the alternative cases in Table I. The correlated systematic uncertainties on the upper limit of Z_s signal yields associated with the fit range, signal shape, ϕ and π^0 mass window requirements, ϕ sideband range, and the $\phi\pi\pi$ PWA model are considered by performing alternative fits and taking the maximum value of N^{UL} as the upper limit, while the uncorrelated systematic uncertainties described in detail later are taken into account by smearing the likelihood curves.

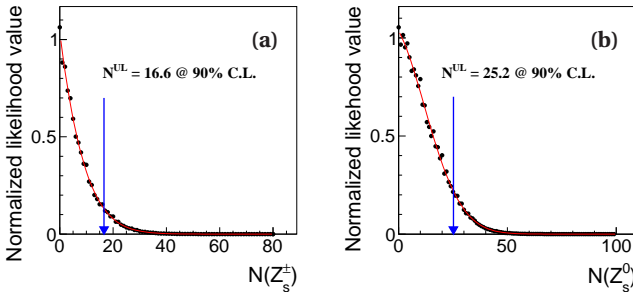


Figure 4. The distributions of the normalized likelihood values versus the number of Z_s events for (a) $e^+e^- \rightarrow \phi\pi^+\pi^-$ and (b) $e^+e^- \rightarrow \phi\pi^0\pi^0$.

The upper limits on the Z_s cross section are calculated

with

$$\sigma_{Z_s}^{\text{UL}}(e^+e^- \rightarrow Z_s\pi, Z_s \rightarrow \phi\pi) = \frac{N^{\text{UL}}}{\mathcal{L}(1+\delta)\epsilon\mathcal{B}}, \quad (1)$$

where \mathcal{L} is the integrated luminosity of the data taken at 2.125 GeV, and determined to be $(108.49 \pm 0.75) \text{ pb}^{-1}$ [14] from large-angle Bhabha scattering events; $(1+\delta)$ is a radiative correction factor calculated to the second-order in QED [23] by assuming that the line shape follows the measured cross section of the BaBar experiment [18], determined as 0.982 and 0.955 for the $e^+e^- \rightarrow \phi\pi^+\pi^-$ and $\phi\pi^0\pi^0$ channels, respectively; ϵ is the efficiency; and \mathcal{B} is either $\mathcal{B}(\phi \rightarrow K^+K^-)$ for $\phi\pi^+\pi^-$ or $\mathcal{B}(\phi \rightarrow K^+K^-) \times \mathcal{B}^2(\pi^0 \rightarrow \gamma\gamma)$ for $\phi\pi^0\pi^0$ [19]. The corresponding upper limits on the cross sections of Z_s production are summarized in Table I.

Table I. Upper limits on the numbers of events, detection efficiencies, and upper limits on the cross sections (in pb) including systematic uncertainties of $e^+e^- \rightarrow Z_s\pi(\rightarrow \phi\pi\pi)$ for the different Z_s mass (in GeV/c^2) and width (in MeV) hypotheses.

| | Γ | M | 1.380 | | | 1.400 | | | 1.420 | | |
|-----------|----------|---|-----------------|----------------|----------------------------|-----------------|----------------|----------------------------|-----------------|----------------|----------------------------|
| | | | N^{UL} | $\epsilon(\%)$ | $\sigma_{Z_s}^{\text{UL}}$ | N^{UL} | $\epsilon(\%)$ | $\sigma_{Z_s}^{\text{UL}}$ | N^{UL} | $\epsilon(\%)$ | $\sigma_{Z_s}^{\text{UL}}$ |
| Z_s^\pm | 0 | 5 | 22.2 | 47.3 | 0.90 | 16.6 | 46.9 | 0.68 | 44.4 | 46.8 | 1.82 |
| | 5 | 5 | 38.0 | 47.5 | 1.54 | 29.8 | 46.9 | 1.22 | 54.4 | 47.2 | 2.21 |
| | 10 | 5 | 49.6 | 47.5 | 2.01 | 40.0 | 47.4 | 1.62 | 60.8 | 47.3 | 2.47 |
| Z_s^0 | 0 | 5 | 25.6 | 13.8 | 3.75 | 25.2 | 13.7 | 3.72 | 27.2 | 13.5 | 4.07 |
| | 5 | 5 | 28.0 | 13.8 | 4.10 | 28.6 | 13.7 | 4.22 | 30.2 | 13.5 | 4.52 |
| | 10 | 5 | 31.2 | 13.8 | 4.57 | 32.4 | 13.7 | 4.78 | 33.6 | 13.6 | 4.99 |

The $e^+e^- \rightarrow \phi\pi\pi$ signal yields are obtained from extended unbinned maximum likelihood fits to the $M(K^+K^-)$ distributions. In the fit, the ϕ peak is modeled as the signal MC simulated shape convoluted with a Gaussian function to account for the mass resolution difference between data and MC simulation, while the background is described by a second-order polynomial function. The fits to $M(K^+K^-)$ spectra, shown in Figs. 1 (a) and (b), yield (9421 ± 138) $\phi\pi^+\pi^-$ and (1649 ± 60) $\phi\pi^0\pi^0$ events. The detection efficiencies are $(52.7 \pm 0.1)\%$ and $(16.0 \pm 0.1)\%$, respectively, obtained from the signal MC samples generated according to the nominal PWA results. The cross sections for $e^+e^- \rightarrow \phi\pi^+\pi^-$ and $e^+e^- \rightarrow \phi\pi^0\pi^0$ are determined to be $(343.0 \pm 5.1) \text{ pb}$ and $(208.3 \pm 7.6) \text{ pb}$, respectively.

Sources of systematic uncertainties and their corresponding contributions to the measurements of the cross sections are summarized in Table II. The uncertainties of the MDC tracking efficiency for each charged kaon and pion and the photon selection efficiency are studied with a control sample $e^+e^- \rightarrow \phi\pi^+\pi^-$ taken at the energy of 2.125 GeV and a control sample of $J/\psi \rightarrow \pi^+\pi^-\pi^0$, respectively, and the differences between data and MC simulation are less than 1.5% per charged track and 1.0% per photon. Similarly, the uncertainties related to the pion and kaon PID efficiencies are also studied with the sample $e^+e^- \rightarrow \phi\pi^+\pi^-$ taken at the energy of 2.125 GeV, and the average differences of the

PID efficiencies between data and MC simulation are determined to be 3% and 1% for each charged kaon and pion, respectively, which are taken as the systematic uncertainties.

Uncertainties associated with kinematic fits come from the inconsistency of the track helix parameters between data and MC simulation. The helix parameters for the charged tracks of MC samples are corrected to eliminate the inconsistency, as described in Ref. [24], and the agreement of χ^2 distributions between data and MC simulation is much improved. We take half of the differences on the selection efficiencies with and without the correction as the systematic uncertainties, which are 2.1% for $\phi\pi^+\pi^-$ and 0.1% for $\phi\pi^0\pi^0$ channels, respectively. The difference of the selection efficiencies associated with the π^0 mass window requirement between data and MC simulation is estimated to be about 0.1%, which is taken as the systematic uncertainty for the mode $e^+e^- \rightarrow \phi\pi^0\pi^0$.

In the measurement of the cross section for $e^+e^- \rightarrow \phi\pi\pi$, the nominal fit range for $M(K^+K^-)$ is $(0.99, 1.09) \text{ GeV}/c^2$. Alternative fits are performed by varying the fitting range. The maximum changes on the calculated cross sections are assigned as the uncertainties from the fitting range. The uncertainties associated with the background shape in the fits to $M(K^+K^-)$ are estimated with alternative fits by changing the second-order polynomial function to a third-order Chebychev polynomial function. Alternative fits to $M(K^+K^-)$ are performed by removing the smeared resolution function to estimate the uncertainties associated with the ϕ signal shape. The resultant differences are assigned as the systematic uncertainties. The uncertainties associated with the signal MC model are estimated with alternative MC samples based on different PWA models, in which the component of $f_0(1370)$ intermediate state is replaced by a phase space process with $J^{PC} = 0^{++}$. The fit can also provide a reasonable description of the data while the likelihood values become slightly worse in both processes. The resultant changes on the efficiency are assigned to be the systematic uncertainties.

The branching fractions of the intermediate processes $\phi \rightarrow K^+K^-$ $[(48.9 \pm 0.5)\%]$ and $\pi^0 \rightarrow \gamma\gamma$ $[(98.823 \pm 0.034)\%]$ are taken from the PDG [19], where the overall uncertainty, 1.1%, is taken as the systematic uncertainty. The luminosity is determined to be $(108.49 \pm 0.75) \text{ pb}^{-1}$ in Ref. [14] with an uncertainty of 0.7%. Uncertainties in the $Y(2125)$ resonance parameters and possible distortions of the $Y(2125)$ line shape introduce small systematic uncertainties in the radiative correction factor and the efficiency. This is estimated using the different line shapes measured by BaBar and Belle, and the difference in $(1 + \delta) \cdot \epsilon$ are taken as a systematic error, 3.1% for $e^+e^- \rightarrow \phi\pi^+\pi^-$ and 1.2% for $e^+e^- \rightarrow \phi\pi^0\pi^0$, respectively.

In summary, a search for a strangeonium-like structure, Z_s , in the process $e^+e^- \rightarrow \phi\pi\pi$ is performed using 108 pb^{-1} of data collected with the BESIII detector at 2.125 GeV. No Z_s signal is observed in the $\phi\pi$ invariant mass spectrum, and corresponding upper limits on the cross sections of Z_s

Table II. Systematic uncertainties (in %) for the measurements of the upper limits (uncorrelated ones) and cross sections. Assuming the uncertainties are uncorrelated, the total uncertainty is the quadratic sum of the individual values.

| Source | Z_s^\pm | $\phi\pi^+\pi^-$ | Z_s^0 | $\phi\pi^0\pi^0$ |
|-----------------------|-----------|------------------|---------|------------------|
| MDC tracking | 4.5 | 4.5 | 1.5 | 1.5 |
| Photon detection | ... | ... | 4 | 4 |
| K PID | 3 | 3 | 3 | 3 |
| π PID | 2 | 2 | ... | ... |
| Kinematic fit | 2.1 | 2.1 | 0.1 | 0.1 |
| π^0 mass window | ... | ... | ... | 0.1 |
| Fitting range | ... | 0.1 | ... | 1.4 |
| Signal shape | ... | 1.3 | ... | 2.2 |
| Background shape | ... | 1.3 | ... | 2.0 |
| Model uncertainty | ... | 0.8 | ... | 1.3 |
| Branching fractions | 1.1 | 1.1 | 1.1 | 1.1 |
| Integrated luminosity | 0.7 | 0.7 | 0.7 | 0.7 |
| ISR | 3.1 | 3.1 | 1.2 | 1.2 |
| Total | 7.0 | 7.3 | 5.5 | 6.5 |

production at the 90% C.L. are determined around the $K^*\bar{K}$ mass threshold (around $1.4 \text{ GeV}/c^2$) with different width hypotheses, as summarized in Table I. The results indicate the ISPE mechanism at $K^*\bar{K}$ threshold is not as significant as predicted in Ref. [15]. Further study with larger statistics is essential to examine the existence of Z_s structure and test the ISPE mechanism.

In addition, the cross sections for $e^+e^- \rightarrow \phi\pi^+\pi^-$ and $e^+e^- \rightarrow \phi\pi^0\pi^0$ are determined to be $(343.0 \pm 5.1 \pm 25.1) \text{ pb}$ and $(208.3 \pm 7.6 \pm 13.5) \text{ pb}$, respectively. The measured cross section for $e^+e^- \rightarrow \phi\pi^+\pi^-$ slightly differs from previous measurements from the BaBar [18] ($510 \pm 50 \pm 21 \text{ pb}$ at 2.1125 GeV) and Belle [25] ($480 \pm 60 \pm 42 \text{ pb}$ at 2.1125 GeV) experiments, but the measurements are still compatible within 3 standard deviations. The cross section for $e^+e^- \rightarrow \phi\pi^0\pi^0$ is consistent with BaBar's measurement [18] ($195 \pm 50 \pm 14 \text{ pb}$ at 2.100 GeV) within uncertainties. For both measurements, the statistical uncertainties are reduced significantly.

The BESIII collaboration thanks the staff of BEPCII and the IHEP computing center for their strong support. This work is supported in part by National Key Basic Research Program of China under Contract No. 2015CB856700; National Natural Science Foundation of China (NSFC) under Contracts Nos. 11235011, 11335008, 11425524, 11625523, 11635010, 11675184, 11735014; the Chinese Academy of Sciences (CAS) Large-Scale Scientific Facility Program; Youth Science Foundation of China under Contract No. Y5118T005C; the CAS Center for Excellence in Particle Physics (CCEPP); Joint Large-Scale Scientific Facility Funds of the NSFC and CAS under Contracts Nos. U1332201, U1532257, U1532258; CAS under Contracts Nos. KJCX2-YW-N29, KJCX2-YW-N45, QYZDJ-SSW-SLH003; 100 Talents Program of CAS; National 1000 Talents Program of China; INPAC and Shanghai Key Laboratory for Particle Physics and Cosmology; German Research Foundation DFG under Contracts Nos. Collaborative Research

Center CRC 1044, FOR 2359; Istituto Nazionale di Fisica Nucleare, Italy; Koninklijke Nederlandse Akademie van Wetenschappen (KNAW) under Contract No. 530-4CDP03; Ministry of Development of Turkey under Contract No. DPT2006K-120470; National Natural Science Foundation of China (NSFC) under Contracts Nos. 11505034, 11575077; National Science and Technology fund; The Swedish Research Council; U. S. Department of Energy under Contracts Nos. DE-FG02-05ER41374, DE-SC-0010118, DE-SC-0010504, DE-SC-0012069; University of Groningen (RuG) and the Helmholtzzentrum fuer Schwerionenforschung GmbH (GSI), Darmstadt; WCU Program of National Research Foundation of Korea under Contract No. R32-2008-000-10155-0.

-
- [1] M. Ablikim *et al.* (BESIII Collaboration), Phys. Rev. Lett. **110**, 252001 (2013).
 - [2] Z. Q. Liu *et al.* (Belle Collaboration), Phys. Rev. Lett. **110**, 252002 (2013).
 - [3] M. Ablikim *et al.* (BESIII Collaboration), Phys. Rev. Lett. **111**, 242001 (2013).
 - [4] M. Ablikim *et al.* (BESIII Collaboration), Phys. Rev. Lett. **112**, 132001 (2014).
 - [5] M. Ablikim *et al.* (BESIII Collaboration), Phys. Rev. Lett. **112**, 022001 (2014).
 - [6] K. Chilikin *et al.* (Belle Collaboration), Phys. Rev. D **90**, 112009 (2014).
 - [7] A. Roel *et al.* (LHCb Collaboration), Phys. Rev. Lett. **112**, 222002 (2014).
 - [8] L. Maiani, V. Riquer, R. Faccini, F. Piccinini, A. Pilloni, and A. D. Polosa, Phys. Rev. D **87**, 111102 (2013).
 - [9] M. Ablikim *et al.* (BESIII Collaboration), Phys. Rev. Lett. **115**, 112003 (2015).
 - [10] M. Ablikim *et al.* (BESIII Collaboration), Phys. Rev. Lett. **113**, 212002 (2014).
 - [11] M. Ablikim *et al.* (BESIII Collaboration), Phys. Rev. Lett. **115**, 182002 (2015).
 - [12] G. J. Ding and M. L. Yan, Phys. Lett. B **650**, 390 (2007).
 - [13] S. Okubo, Phys. Lett. **5**, 165 (1963); G. Zweig, CERN Report No. 8419/TH412, 1964; J. Iizuka, Prog. Theor. Phys. Suppl. **37**, 21 (1966).
 - [14] M. Ablikim *et al.* (BESIII Collaboration), Chin. Phys. C **41**, 113001 (2017).
 - [15] D. Y. Chen, X. Liu, and T. Matsuki, Eur. Phys. J. C **72**, 2008 (2012).
 - [16] M. Ablikim *et al.* (BESIII Collaboration), Nucl. Instrum. Methods Phys. Res., Sect. A **614**, 345 (2010).
 - [17] S. Agostinelli *et al.*, Nucl. Instrum. Methods Phys. Res., Sect. A **506**, 250 (2003).
 - [18] J. P. Lees *et al.* (BaBar Collaboration), Phys. Rev. D **86**, 012008 (2012).
 - [19] C. Patrignani *et al.* (Particle Data Group), Chin. Phys. C **40**, 100001 (2016).
 - [20] B. S. Zou and D. V. Bugg, Eur. Phys. J. A **16**, 537 (2003).
 - [21] M. Ablikim *et al.* (BES Collaboration), Phys. Lett. B **607**, 243 (2005).
 - [22] M. Ablikim *et al.* (BES Collaboration), Phys. Lett. B **598**, 149 (2004).
 - [23] E. A. Kuraev and V. S. Fadin, Yad. Fiz. **41**, 733 (1985) [Sov. J. Nucl. Phys. **41**, 466 (1985)]; R. G. Ping, Chin. Phys. C **38**, 083001 (2014).
 - [24] M. Ablikim *et al.* (BESIII Collaboration), Phys. Rev. D **87**, 012002 (2013).
 - [25] C. P. Shen *et al.* (Belle Collaboration), Phys. Rev. D **80**, 031101 (2009).